Title: Hormonal regulation of Semaphorin 7a in ER+ breast cancer drives therapeutic resistance

Authors: Lyndsey S Crump[1,2], Garhett Wyatt[3], Taylor R Rutherford[1,2], Jennifer K Richer[4], Weston W Porter[3], and Traci R Lyons[1,2,5]

Affiliations: [1]Division of Medical Oncology, Department of Medicine, School of Medicine, University of Colorado Anschutz Medical Campus, Aurora, CO, USA; [2]Young Women's Breast Cancer Translational Program, University of Colorado Anschutz Medical Campus, Aurora, CO 80045, USA. [3]Department of Veterinary Integrative Biosciences, Texas A&M University, College Station, TX, USA; [4]Department of Pathology, School of Medicine, University of Colorado Anschutz Medical Campus, Aurora, CO, USA; [5]University of Colorado Cancer Center, Aurora, CO, 80045, USA

Running Title: Semaphorin 7a in ER+ breast cancer

Keywords: breast cancer, semaphorin 7a, endocrine therapy, resistance

Additional Information:

Financial Support: This work was supported by Colorado Clinical and Translational Sciences Institute Grant TL1 TR001081 (to L.S.C.), National Institutes of Health Grants F31 CA236140 (to L.S.C./T.R.L), NIH/NCI R01 CA211696-01A1 (to T.R.L.), CU Anschutz RNA Bioscience Initiative RNA-seq Pilot Grant Program (to T.R.L), NIH/NICHD R01-HD083952-01 (to W.W.P), NIH/NCI R01 CA187733-01 (to J.K.R), NIH/NCI R21-CA197896 (to W.W.P), DOD BCRP W81XWH-16-1-0422 (to J.K.R), ACS RSG-16-171-010CSM (to T.R.L.), and Department of Medicine Outstanding Early Career Scholars Award (to T.R.L.).

Corresponding author: Traci R Lyons, University of Colorado Anschutz Medical Campus, Department of Medicine/Medical Oncology, MS8117, RC1S-8106, 12801 East 17th Ave, Aurora, CO 80045, traci.lyons@cuanschutz.edu

Disclosure Summary: The authors have nothing to disclose.

Word count: 6,025

Number of figures: 6

Number of tables: 0

ABSTRACT

Approximately 70% of all breast cancers are estrogen receptor positive (ER+BC) and endocrine therapy has improved survival for patients with ER+BC. Yet, up to half of these tumors recur within 20 years. Recurrent ER+BCs develop resistance to endocrine therapy; thus, novel targets are needed to treat recurrent ER+BC. We found that semaphorin 7A (SEMA7A) confers significantly decreased patient survival rates in ER+BC. We show that *SEMA7A* is hormonally regulated in ER+BC, but its expression does not uniformly decrease with anti-estrogen treatments. Additionally, overexpression of SEMA7A in ER+ cell lines drives increased *in vitro* growth in the presence of estrogen-deprivation, tamoxifen, and fulvestrant. In *in vivo* studies, we found that SEMA7A confers primary tumor resistance to fulvestrant and, importantly, induced lung metastases. Finally, we identify pro-survival signaling as a therapeutic vulnerability of ER+SEMA7A+ tumors and propose that targeting with inhibitors of survival signaling such as venetoclax may have efficacy for treating SEMA7A+ tumors.

SIGNIFICANCE

We report that SEMA7A predicts for, and likely contributes to, poor response to standard-of-care therapies and suggest that patients with SEMA7A+ER+ tumors may benefit from alternative therapeutic strategies.

INTRODUCTION

Breast cancer (BC) is the most commonly diagnosed cancer and the second leading cause of cancer-associated death in women in the United States. Estrogen receptor positive (ER+) BCs comprise approximately 70% of all BC cases. The development of effective anti-estrogen-based endocrine therapies, including aromatase inhibitors (AI) and selective estrogen receptor modulators (e.g., tamoxifen) or degraders (e.g., fulvestrant/Faslodex) has facilitated the successful treatment of ER+ primary tumors. However, depending on nodal involvement, 22-52% of women with ER+BC will experience disease recurrence within 20 years (1), frequently in a distant metastatic site, such as lung, liver, bone, or brain. These recurrent ER+BCs uniformly develop resistance to endocrine therapies, rendering most therapeutic interventions in the clinical setting ineffective at preventing metastatic outgrowth. Therefore, novel molecular targets are needed to predict for and treat recurrent and/or metastatic ER+BCs.

Semaphorin 7a (SEMA7A) is a glycosylphosphatidylinositol-anchored member of the semaphorin family of signaling proteins. SEMA7A has well-described roles in the promotion of axon guidance, immune modulation, and cellular migration (2-6). In adults, SEMA7A is expressed in the brain, bone marrow, lung, and skin, but is minimally expressed in many adult tissues, including the mammary gland (information via https://www.proteinatlas.org). Interestingly, in neuronal cells of the hypothalamus, SEMA7A expression is regulated by steroid hormones (7), while in pulmonary fibrosis models, SEMA7A is regulated by TGF-β (8). In its normal physiological role, SEMA7A binds β1-integrin to activate downstream signaling cascades, including pro-invasive MAPK/ERK and pro-survival PI3K/AKT pathways (2,5,8). Our group and others have described tumor-promotional roles for SEMA7A in mammary cancers, including tumor and host derived mechanisms of increased tumor growth, cellular migration, epithelial to mesenchymal transition, immune cell infiltration, remodeling of the blood and lymphatic vasculature, and metastatic spread (9-13). More recently, it has been reported that SEMA7A expression in lung cancer confers resistance to EGFR tyrosine kinase inhibition (14).

Studies to date have investigated the role of SEMA7A in BC using pre-clinical models of triple negative BC (TNBC), which lack expression of ER (ER-), progesterone receptor (PR-), and amplification of HER2 (HER2-). Specifically, our studies in TNBC reveal that SEMA7A

promotes TNBC cell growth, invasion, lymphangiogenesis, lymph vessel invasion, and metastasis (10,15). However, our previous genomics analysis in patient datasets demonstrated that *SEMA7A* expression correlates with poor prognosis in patients with both ER- and ER+BC and that *SEMA7A* expression levels were highest in luminal A tumors, which are generally ER+ and/or PR+ and HER2- (9). Thus, understanding the role of SEMA7A in ER+BC is critical for a complete understanding of its role and impact on BC progression. Our results presented herein show that *SEMA7A* mRNA expression is highest in patients with ER+ BC and that SEMA7A induces pleiotropic tumor-promotional effects in ER+BC cells. We also describe a novel relationship between hormone signaling and expression of SEMA7A in BC. Additionally, we report for the first time that expression of SEMA7A confers resistance to standard-of-care endocrine therapy and to CDK 4/6 inhibition in pre-clinical ER+ models. Finally, using pre-clinical models, we identify a therapeutic vulnerability of SEMA7A-expressing tumors with the BCL2 inhibitor, venetoclax (ABT-199/GDC-0199). These data provide promising evidence that SEMA7A+ER+BCs that do not respond to endocrine therapies may respond to novel treatment regimens in the clinic.

MATERIALS AND METHODS

Cell culture

MCF7 cells were obtained from K. Horwitz (University of Colorado Anschutz Medical Campus). T47D and BT474 cells were obtained from V. Borges and M. Borakove (University of Colorado Anschutz Medical Campus). MCF10DCIS cells were obtained from K. Polyak and A. Marusyk (Harvard University, Cambridge, MA). MDA-MB-231 cells were obtained from P. Schedin (Oregon Heath and Sciences University, Portland OR). Tamoxifen resistant T47D cells were obtained from A. Ward and C. Sartorius (University of Colorado Anschutz Medical Campus). Cell lines were validated by fingerprinting analysis at the University of Colorado Anschutz Medical Campus Molecular Biology Core. Cells were routinely tested for mycoplasma contamination throughout the studies described herein with either Lonza MycoAlert PLUS (Walkersville, MD) or Mycoflour Mycoplasma Detection Kit (Molecular Probe, Eugene OR). Cells were cultured at 37 °C and 5% CO2. MCF7 and BT474 cells were grown in MEM with 5% heat-inactivated fetal bovine serum (FBS; Atlanta Biologicals, Flowery Branch, GA) and 1%

118 penicillin/streptomycin (P/S; ThermoFisher Scientific). T47D and E0771 cells were grown in
119 RPMI 1640, with 10% heat-inactivated FBS and 1% P/S. Experiments were performed with
120 cells under passage 30. Forced suspension cultures were performed by coating plates with
121 12 mg/ml poly-2-hydroxyethyl methacrylate (Sigma, St. Louis, MO). For exogenous SEMA7A
122 treatments, SEMA7A was purified from SEMA7A-Fc expressing MDA-MB-231 cells in
123 collaboration with the CU Anschutz Medical Campus Protein Purification/MoAB/Tissue Culture
124 Core.

125 **Transfections**

126 For knockdown studies, SEMA7A-targeting shRNA plasmids (shSEMA7A KD1 and KD2) or a
127 scrambled control (Scr; SA Biosciences, Frederik, MD, and the Functional Genomics Facility at
128 the CU Anschutz Medical Campus) were transfected using X-tremeGENE transfection reagent
129 (Millipore Sigma, St. Louis, MO) as described by the manufacturer. SEMA7A overexpression in
130 MCF7 cells was achieved using a SEMA7A-Fc plasmid (generous gift from R. Medzhitov, Yale
131 University, New Haven, CT). A pcDNA3.1 empty vector control plasmid was obtained from H.
132 Ford (CU Anschutz Medical Campus). All other plasmids were obtained from the Functional
133 Genomics Core at the University of Colorado Anschutz Medical Campus. Knockdown and
134 overexpression were confirmed via qPCR and Western blot analysis.

135 **Luciferase Reporter Assay**

136 The reporter construct was generated by cloning a -820 to +182 base pair fragment of the
137 *SEMA7A* promoter into the pGL3-Basic Luciferase reporter (Invitrogen). The four mutations for
138 the ERE1/2 sites were as follows: TGACCC ->TGTTCC, GGGTCC -> GCATCC, GGGTCA ->
139 GCATCA, GGGCGG -> TTACAG. Three SP1 sites were mutated: GGGCGG -> TTACAG.
140 50,000 cells were seeded in a 12-well plate and incubated for 5 minutes with 50µL Opti-MEM
141 (Invitrogen, Carlsbad, CA) and 3µL GeneJuice (Millipore Sigma, Burlington, MA) per well. 0.5-
142 1µg of DNA was added to GeneJuice Transfection Reagent/serum-free medium mixture. Cells
143 were harvested 48 hours after transfection using Reporter Lysis Buffer (Promega, Madison,
144 WI), unless treated with 10nM E2 . If treated with E2, cells were serum starved for 48 hours in
145 serum-free medium. Cells were then treated with 10nM E2 for 48 hours and harvested as
146 stated above. Luciferase activity was normalized to total protein.

147 **Drug and Hormone Treatments**

148 Fulvestrant, 4-hydroxytamoxifen, and 17-β estradiol (E2) were purchased from Millipore Sigma
149 (St. Louis, MO). For *in vitro* hormone treatments, cells were cultured in charcoal-stripped
150 serum (Thermo Scientific, Waltham, MA) containing phenol red-free media for 3-5 days, then
151 treated with 10nM E2 as determined by our dose response and the literature(16-18). For
152 clonogenic and growth assays, fulvestrant and 4-hydroxytamoxifen treatments were at a final
153 concentration of 7.5nM and 5μM, respectively. Palbociclib and SU6656 were acquired from
154 MedChemExpress (Monmouth Junction, NJ) and treatments were at a final concentration of
155 2.5μM and 5μM, respectively, in DMSO. LY294002 was purchased from Cell Signaling
156 Technologies (Danvers, MA) and *in vitro* treatments were at a final concentration of 2.5μM
157 LY294002 in DMSO. *In vitro* venetoclax (Abbvie, Chicago, IL) was at a final concentration of
158 300nM in DMSO.

159 **Cell Growth, Invasion, and Death Assays**

160 100,000 MCF7 cells were seeded per well of a 6-well dish to assess growth *in vitro*. Cells were
161 fixed with 10% NBF and stained with crystal violet at the indicated time points. 1,000 MCF7
162 cells or 5,000 T47D cells were seeded per well of a 6-well dish and assessed 7-14 days later
163 for clonogenic assays. 3D matrigel and collagen cultures were performed as previously
164 described (9,19). Cleaved caspase 7 was measured using a Caspase Glo assay (Promega,
165 Madison, WI) as described by the manufacturer. Exogenous SEMA7A treatments were at a
166 final concentration of 5μg/mL.

167 **RNA isolation**

168 RNA was isolated using the commercially available Quick-RNA kit (Zymo Research, Irvine,
169 CA). RNA concentration and purity were assessed using a Nanodrop machine via absorbance
170 at 280 nm, 260 nm, and 230 nm. 1μg of RNA was used to synthesize cDNA with the Bio-Rad
171 (Hercules, CA) iScript cDNA Synthesis kit with the following conditions: 25ºC for 5 min., 42ºC
172 for 30 min., and 85ºC for 5 min.

173 **mRNA and protein expression analysis**

174 cDNA was quantified via qPCR using Bio-Rad iTaq Universal SYBR Green Supermix and
175 primers for *SEMA7A* (Bio-Rad PrimePCR, Hercules, CA) using the following conditions: 95ºC
176 for 3 min, then 40 cycles of 95ºC for 15 sec and 60ºC for 1 min, 95ºC for 30 sec, and 55ºC for
177 1 min. Primer fidelity was assessed for each qPCR experiment using a 95ºC melt curve.
178 *SEMA7A* mRNA was detected with Bio-Rad primers (forward: CTCAGCCGTCTGTGTGTATT,
179 reverse: CTCAGGTAGTAGCGAGAGTTTG). Primers for *ESR1 (forward: 5-*
180 *GAACCGAGATGATGTAGCCA, reverse: GTTTGCTCCTAACTTGCTCTTG)* and *PGR*
181 *(forward: ATTTCATCCACGTGCCTATCC, reverse: CCTTCCTCCTCCTCCTTTATCT)* were
182 purchased from IDP. mRNA quantification was normalized using the geometric average of two
183 reference genes: *GAPDH* (forward: CAAGAGCACAAGAGGAAGAGAG, reverse:
184 CTACATGGCAACTGTGAGGAG) and *RPS18* (forward: GCGAGTACTCAACACCAACA,
185 reverse: GCTAGGACCTGGCTGTATTT). Data were analyzed using the relative standard
186 curve method.

187 Western blots were performed by loading equal amounts of protein lysates as determined by
188 Bradford assay. Samples were separated on a 10% tris-glycine SDS polyacrylamide gel and
189 electroblotted onto a polyvinylidene fluoride membrane. SEMA7A blots were probed with anti-
190 SEMA7A (clone C6, Santa Cruz Biotechnologies, Dallas, TX) and goat-anti-mouse secondary
191 (Abcam, Cambridge, MA). Blots were then exposed and developed on film. Color images were
192 converted to black and white for presentation, and, if applied, color corrections were applied
193 uniformly to all lanes of the blot to ease viewing of bands. No nonlinear intensity or color
194 adjustments to specific features were performed. Multiple replicates were performed for each
195 blot, and representative blots with corresponding quantifications normalized to loading controls
196 are shown where appropriate.

197 **Animal models**

198 2,500,000 SEMA7A overexpressing or empty vector control MCF7 cells were injected into the
199 #4 mammary fat pads of 6-7 week old female, estrogen supplemented (20), NSG mice
200 (Jackson Laboratory, Bar Harbor, ME) or NCG mice (Charles River, Wilmington, MA). Tumors
201 were measured using digital calipers every 3-4 days, and tumor volume was calculated as (L x
202 W x W x 0.5). For estrogen independent studies, animals received sham beeswax pellets. For
203 drug treatment studies, fulvestrant dosing began when average tumor volume reached

204 ~200mm^2 with the following dosing regimen: 2.5mg fulvestrant in 10% ethanol and 90%
205 sesame oil, injected subcutaneously every 5 days. This dose is equivalent to approximately
206 83mg/kg per mouse and, using the FDA Dosing Guidance for Industry: Conversion of Animal
207 Doses to Human Equivalent Doses, equivalent to 6.7mg/kg in humans. For venetoclax studies,
208 venetoclax was dissolved in phosal-50G:polyethylene glycol-400:ethanol at 6:3:1 to a final
209 concentration of 12mg/mL and administered via oral gavage. Tumors were harvested at
210 designated study endpoints. Mammary glands with intact tumor and lungs were harvested,
211 formalin fixed, and paraffin embedded for immunohistochemical analysis. All animal studies
212 were performed under the approval of the University of Colorado Anschutz Medical Campus
213 Institutional Animal Care and Use Committee.

214 **Immunohistochemistry**

215 Tissues were formalin-fixed and paraffin-embedded as previously described (21). Antibody
216 information is provided in STable 1. For staining quantification, slides were scanned into the
217 Aperio Image Analysis software (Leica, Buffalo Grove, IL). The total tumor area was quantified
218 by removing necrotic and stromal areas. Custom algorithms for specific stains were used to
219 quantify stain intensity or percent positive stain as assessed by percent weak, medium, and
220 strong determined using the color-deconvolution tool.

221 **Data Mining Analyses**

222 Kaplan Meir Plotter (22) was used to assess relapse-free survival (RFS) data for 5,143 BC
223 patients with mean follow-up of 69 months. SEMA7A was queried and stratified into high and
224 low expression groups using the auto select best cutoff level function. The generated data
225 were exported, graphed, and analyzed in Graphpad Prism to calculate hazard ratio (HR) with
226 95% confidence intervals and log rank P values. The Gene Expression Based Outcome for
227 Breast Cancer Online platform (http://co.bmc.lu.se/gobo/) was used to query *SEMA7A*
228 expression in 1,881 available sample tumors and a panel of 51 BC cell lines. Data were
229 stratified as high and low SEMA7A based on median expression and reported by molecular
230 subtype. Outcomes data were reported only in patients with ER+BC. The Oncomine Platform
231 (https://www.oncomine.org) was used to query *SEMA7A* in available BC datasets. The p-
232 value threshold was set to 0.05. All fold-changes and gene ranks were accepted. Data are

233 reported from the molecular subtype analysis, correlation with stage and grade, and drug
234 sensitivity screens.

235 **IncuCyte Assay**

236 5,000 SEMA7A overexpressing or empty vector control MCF7 cells were seeded per well in a
237 96 well plate and allowed to adhere overnight. Media was replaced with fresh drug or vehicle
238 treated media the next morning. Drug treatments included 7.5nM fulvestrant, 5μM 4-
239 hydroxytamoxifen, 2.5μM palbociclib, 10μM LY294002, 5μM Su6656, and growth was
240 assessed in an IncuCyte live cell analysis system at the University of Colorado Cancer Center
241 Tissue Culture Core. Confluence was reported every 4 hours.

242 **Generation of Drug Resistant and Estrogen Deprived Cell Lines**

243 Fulvestrant resistant cell lines were generated by injecting 2,500,000 SEMA7A overexpressing
244 or empty vector control MCF7 cells were injected into contralateral #4 mammary fat pads of a
245 6 week old female, estrogen supplemented (20) NCG mouse (Charles River, Wilmington, MA).
246 Fulvestrant treatments began 7 days later with the following dosing regimen: 2.5mg fulvestrant
247 in 10% ethanol and 90% sesame oil, injected subcutaneously every 5 days. 48 days after
248 implantation, tumors were harvested and minced in digestion mixture: MCF7 media with
249 500units/mL collagenase type II and IV, 20μg/mL DNase (Worthington Biochemical,
250 Lakewood, NJ), and 1X Antibiotic-Antimycotic (ThermoFisher, Waltham, MA). Disassociation
251 mixture was incubated at 37°C for one hour. Dissociated cells were centrifuged at 1500 RPM
252 for 7 minutes, then resuspended and plated in standard culture media with 1X Antibiotic-
253 Antimycotic and returned to the incubator overnight. The next day, 7.5nM fulvestrant was
254 added to the media and cells were maintained in these culture conditions. *Ex vivo* fulvestrant
255 resistance was confirmed with clonogenic assays as described above.

256 Long-term estrogen deprived (LTED) cells were cultured in phenol red-free media (MEM for
257 MCF7 and RPMI-1640 for T47D) supplemented with 5% dextran charcoal stripped FBS for 6
258 months.

259 **Drug titration studies**

260 4,000 SEMA7A overexpressing or empty vector control MCF7 cells were seeded per well in a
261 96 well plate and allowed to adhere for 6 hours. Vehicle or increasing concentrations of 4-
262 hydroxytamoxifen or fulvestrant were added. Growth was assessed in BioSpa live cell imaging
263 system (BioTek, Winooski, VT). Confluence was reported every 4 hours.

264 **ELISA**

265 Estradiol ELISA kit (Cayman Chemical, Ann Arbor, MI) was used to measure serum estradiol
266 levels from estrogen supplemented or sham beeswax pellet control mice according to the
267 manufacturer instructions.

268 **Flow Cytometry**

269 MCF7 cells were enzymatically dissociated in Accutase cell detachment solution [Stem cell
270 technology: cat# 07920] for approximately 10 minutes at 37°C. Single cells were stained with
271 anti-mouse/human CD44-AF647 [Biolegend: cat# 103018] and anti-human CD24-FITC
272 [Biolegend: cat# 311104] for 30 minutes at 4°C in the dark. Cells were analyzed on the YETI-
273 ZE5 flow cytometer and data were analyzed using Kaluza software. Cells were delineated from
274 debris by SSC-A/FSC-A and singlets identified by FSC-H/FSC-A. Single cells were
275 subsequently assessed for CD44/CD24 expression.

276 **Statistical analysis**

277 All cell line and xenograft experiments were performed in biological duplicate or triplicate. Data
278 are expressed as means ± SEM for animal studies and ± SD for *in vitro* studies. All statistical
279 analyses were performed on raw data. An unpaired two-tailed student's t test was performed
280 for analyses comparing two groups, while a one-way ANOVA followed by a Tukey–Kramer test
281 was used for multiple comparisons of groups of 3 or more. For tumor volume data and incucyte
282 analyses, a repeated measures one-way ANOVA was used. For Kaplan–Meier analyses, the
283 p-value was determined using a log-rank test. All p-values less than or equal to 0.05 were
284 considered statistically significant, and all statistical analyses were performed in GraphPad
285 Prism 7.01 (San Diego, CA).

286 **RESULTS**

287 **SEMA7A is expressed in ER+ breast cancers and confers poor prognosis**

288 To determine if SEMA7A is expressed in ER+BC, we assessed *SEMA7A* mRNA expression
289 using the Gene Expression-based Outcome for Breast Cancer Online (GOBO) tool. We
290 observed that 67% of luminal subtype cell lines, which are typically ER+, exhibit increased
291 *SEMA7A* expression versus 36-50% of the basal subtypes (which are typically ER-; Figure
292 1A). Average expression was higher when ER+ cell lines were compared to TNBC cell lines
293 and when luminal cell lines were compared to basal subtype (Figure 1B). *SEMA7A* mRNA
294 expression is also increased in ER+ patient tumors (Figure 1C), and we confirmed that
295 *SEMA7A* was overexpressed and/or had a higher copy number rank in ER+ or PR+ disease in
296 7 additional datasets using Oncomine (STable 2). Additionally, *SEMA7A* was highest in stage
297 III and IV, grade 2 and 3, and lymph node positive (LN+) disease in multiple datasets (STable
298 3). We next examined a role for *SEMA7A* status in predicting outcomes for patients with
299 ER+BC; patients with high tumor expression of *SEMA7A* had decreased overall and distant
300 metastasis free survival (Figure 1D-E and SFigure 1A-B). Additionally, using KM Plotter, we
301 further stratified relapse-free survival by LN positivity in the ER+(HER2+/-) subset and
302 observed that high SEMA7A is associated with decreased relapse free survival in patients with
303 both LN+ and LN- status (Figure 1F-G). In fact, the hazard ratio for patients whose tumors
304 were ER+(HER2+/-) SEMA7A+ and with LN- status was the highest. We then confirmed
305 SEMA7A protein expression in ER+ lines (MCF7, T47D, BT474), ER- lines (DCIS, MDA-MB-
306 231, SUM159), and breast epithelial cells derived from human fibrocystic disease (23)
307 (MCF10A) via immunoblot analysis. SEMA7A expression was observed in two of the three
308 ER+ cell lines and one of the three ER- when compared to MCF10A cells (SFigure 1C).

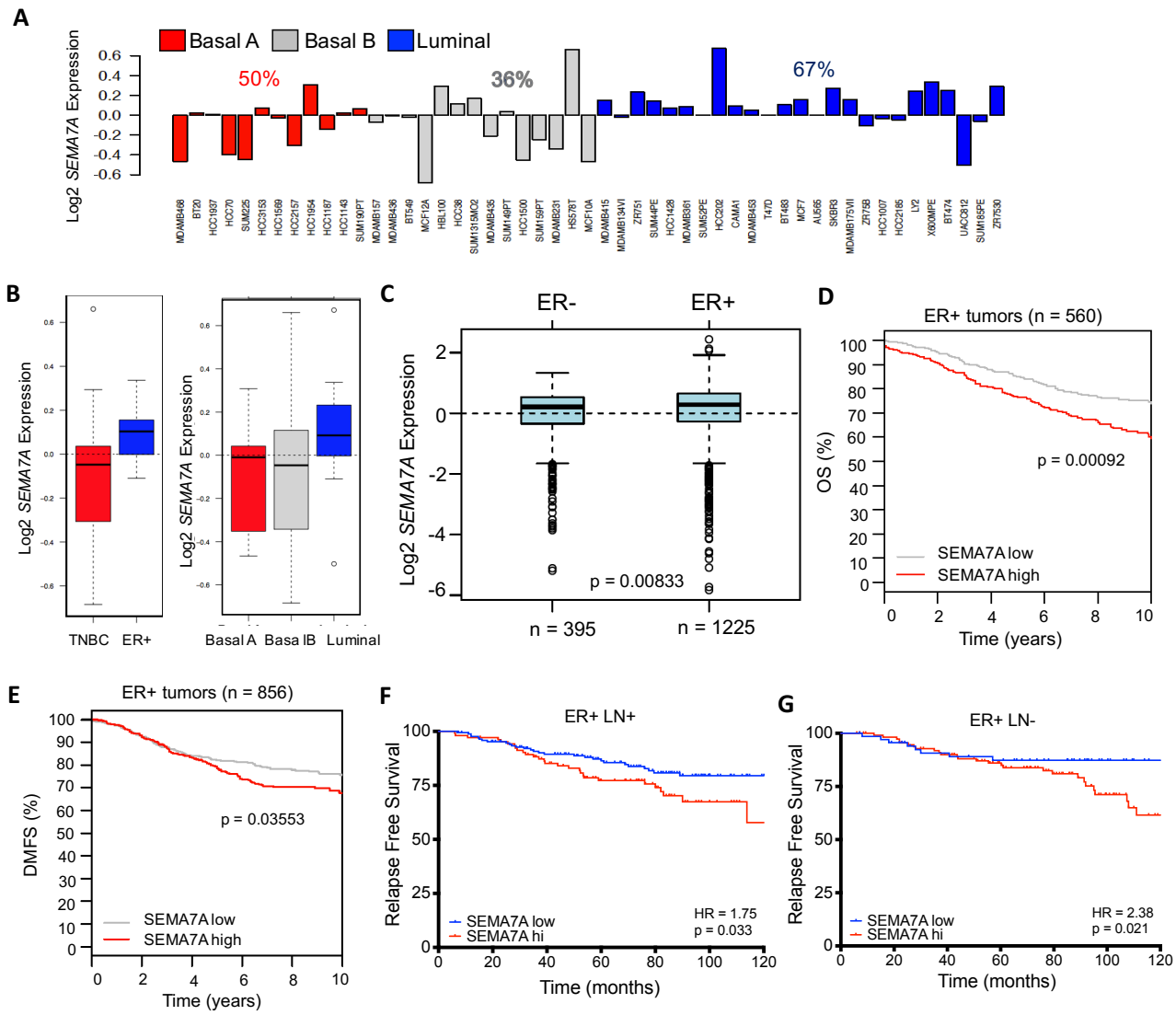

Figure 1: *SEMA7A* is expressed in ER+ breast cancer and associated with poor prognosis. (A-B) The Gene Expression-Based Outcome dataset was assessed for *SEMA7A* mRNA expression levels in basal/triple negative breast cancer (TNBC) and luminal/ER+ breast cancer cell lines (n = 51) and **(C)** in ER- or ER+ patient tumors (n = 1620). In the ER+ subset, **(D)** overall survival (OS) and **(E)** distant metastasis free survival (DMFS) curves are stratified by *SEMA7A* high (red) and low (grey) expression. **(F)** Relapse free survival curves for patients with ER+ and PR+ disease and either lymph node positivity (LN+; n = 277) or **(G)** negativity (LN-; n = 185) are stratified by high *SEMA7A* (red) and low *SEMA7A* (blue) using KMplotter mRNA gene chip data. Hazard ratios (HR) are included.

SEMA7A is regulated by estrogen in breast cancer cells and correlates with relapse in patients with ER+ breast cancer

To test the hypothesis that SEMA7A expression could be induced by estrogen (E2) stimulation, we treated ER+BC cells in estrogen deprived conditions with increasing, physiologically relevant (24), concentrations of estrogen. In both MCF7 and T47D cells, E2 resulted in increased SEMA7A protein expression (Figure 2A-B). Then, to determine whether

316 *SEMA7A* expression could be promoted by ER dependent transcription, we performed an *in*
317 *silico* analysis of the *SEMA7A* promoter using the ConTra (conserved transcription factor
318 binding site) web server (25). We identified two highly conserved estrogen response element
319 (ERE) half sites adjacent to two specificity protein 1 (SP1) consensus binding sites (Figure
320 2C). SP1 has been shown to facilitate ER binding to ERE half sites in gene promoter regions
321 to promote transcription of estrogen target genes (26); thus, we then utilized a *SEMA7A*
322 luciferase reporter construct to measure promoter activity with E2 treatment and observed
323 increased luminescence with 10nM E2 (Figure 2D). We also observed increased *SEMA7A*
324 mRNA after treatment with 10nM E2 (SFigure 2A). Next, we performed luciferase reporter
325 assays with constructs containing point mutations in the ERE and SP1 sites to show that both
326 are required for induction of *SEMA7A* promoter activity by E2 (Figure 2E-F). To determine
327 whether SEMA7A expression was dependent upon ER, we treated MCF7 and T47D cells with
328 fulvestrant, which decreased expression, but was not sufficient to completely block expression
329 of SEMA7A under normal growth conditions (Figure 2G). Then, to mimic conditions resulting
330 from AI therapy, we tested whether long term estrogen deprivation (LTED) of MCF7 and T47D
331 cells would result in downregulation of SEMA7A. Surprisingly, the cells that were deprived of
332 estrogen exhibited marked upregulation of SEMA7A compared to the wildtype (WT) controls
333 (Figure 2H). Additionally, T47D cells that are tamoxifen resistant (TAMR) exhibit upregulation
334 of SEMA7A (Figure 2I). These results suggest that E2 induces *SEMA7A* expression, but that
335 *SEMA7A* expression can also bypass estrogen dependence. Consistent with this, we observe
336 that MCF7 cells, which normally require estrogen supplementation for growth *in vivo*, can grow
337 in the absence of estrogen supplementation when SEMA7A is overexpressed (Figure 2J;
338 SFigure 2B-C).

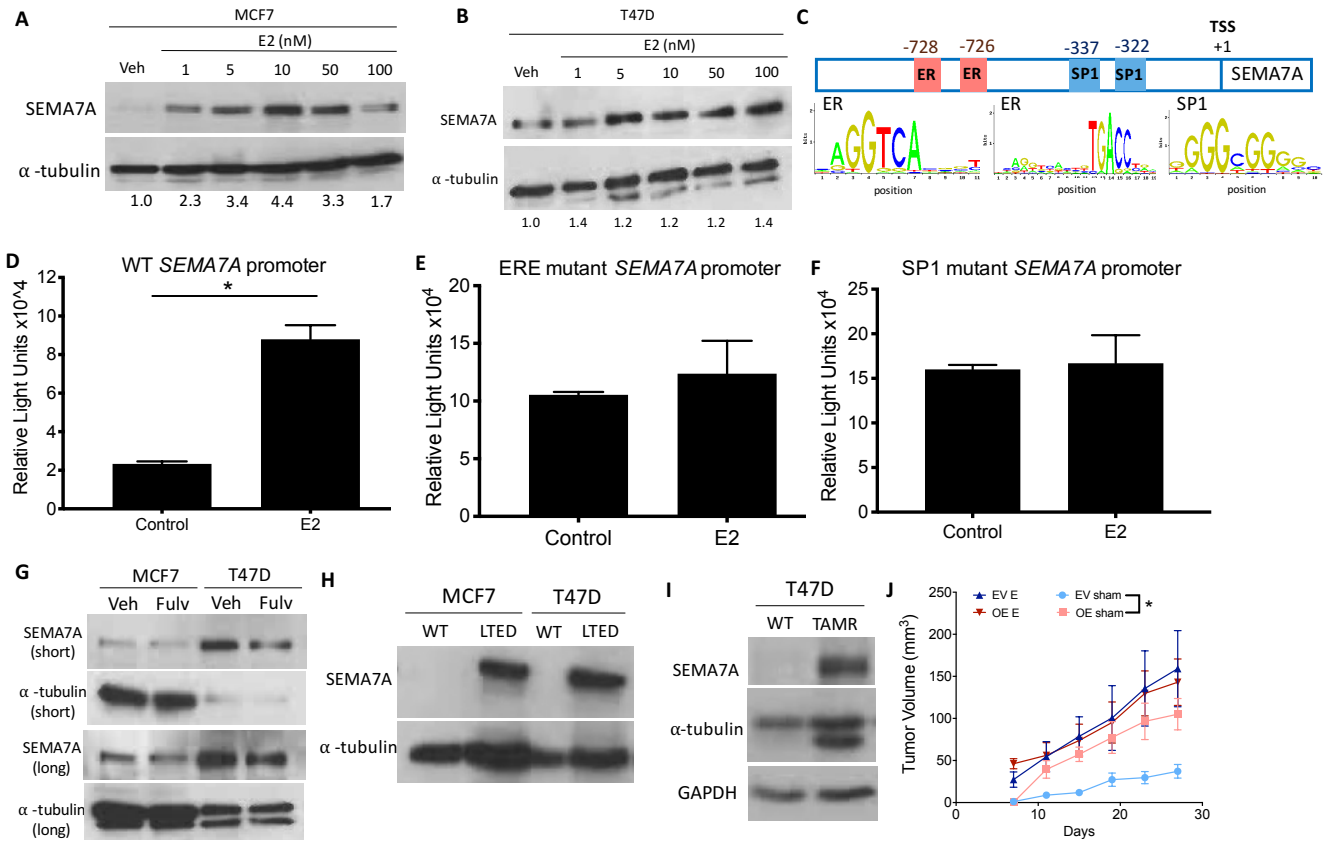

Figure 2: Expression of *SEMA7A* is hormonally regulated. (A) MCF7 and **(B)** T47D cells were grown in charcoal stripped conditions for 3 days, then treated with vehicle or increasing concentrations of estrogen (E2). Representative immunoblots for SEMA7A and α-tubulin are shown (n = 3). Normalized quantifications are shown under each blot. **(C)** A ConTra analysis revealed conserved ER and SP1 binding sites in the *SEMA7A* promoter. Distance from the transcriptional start site (TSS) is noted. **(D)** Luciferase activity in MCF7 cells transfected with a luciferase reporter containing the wildtype (WT) *SEMA7A* promoter, **(E)** an estrogen response element (ERE) mutant *SEMA7A* promoter, or **(F)** an SP1 binding site mutant *SEMA7A* promoter upstream of the luciferase gene, then treated with 10nM estrogen or vehicle control (n = 3 for each panel). **(G)** MCF7 and T47D cells were treated with 7.5nM fulvestrant for 72 hours. Representative SEMA7A and α-tubulin levels are shown via immunoblot with short and long film exposures (n = 3). **(H)** Representative SEMA7A and α-tubulin levels are shown via immunoblot for WT or long term estrogen deprived (LTED) MCF7 and T47D cells (n = 3), and **(I)** WT or tamoxifen resistant (TAMR) T47D cells (n = 3). **(J)** Tumor volumes for empty vector (EV) or SEMA7A overexpressing (OE) MCF7 tumors in hosts with estrogen pellets (E) or sham controls (n = 6/group). *p < 0.05 by unpaired two-tailed t-test (D) or ANOVA with Tukey's multiple comparison test (J)

SEMA7A induces growth and confers therapeutic resistance in ER+ breast cancer cells

To determine if SEMA7A promotes ER+BC progression via increasing tumor cell viability or proliferation, we engineered MCF7 cells to overexpress *SEMA7A*. We confirmed a 3.6-fold increase in SEMA7A protein (SEMA7A OE; Figure 3A) and observed increased cell growth in two-dimensional cultures (Figure 3B), clonogenic assays (Figure 3C), and increased BrdU incorporation in a 3D organoid system that we have previously characterized to model tumor cell growth and invasion into the surrounding tissue (27), which contains Matrigel to model the basement membrane and collagen, which is required for tumor cell invasion (Figure 3D). We also generated two independent shRNA mediated knockdown (KD) variants of SEMA7A and confirmed decreased SEMA7A protein in MCF7 cells (Figure 3E; SFigure 2D). We observed

that SEMA7A KD cells were less confluent over a 72 hour time course (Figure 3F), exhibited decreased colony formation in a clonogenic assay (Figure 3G) and SEMA7A KD 3D organoids have significantly reduced proliferation via BrdU incorporation (Figure 3H).

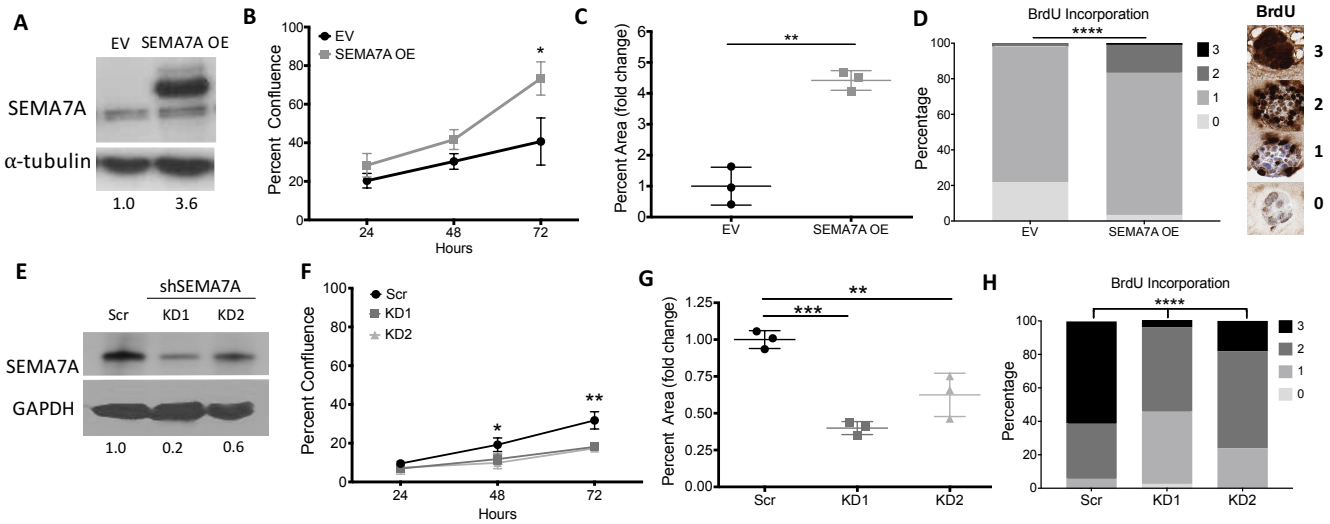

Figure 3: SEMA7A promotes growth of ER+ cells in 2D and 3D cultures. (A). Representative immunoblot for SEMA7A and α-tubulin in MCF7 cell transfected with an empty vector (EV) control or SEMA7A overexpressing (SEMA7A OE) plasmid. Normalized quantifications are shown below (n = 3). **(B)** Confluence of EV or SEMA7A OE MCF7 cells at 24, 48, and 72 hours post seeding (n = 3). **(C)** Clonogenicity of EV or SEMA7A OE MCF7 cells. SEMA7A OE values are normalized to EV controls (n = 3). **(D)** BrdU incorporation was assessed in EV and SEMA7A OE MCF7 cells embedded in Matrigel plus 20% collagen after 5 days in culture. Each organoid received a score 0-3 based on the percent positive of each organoid, where 0 = no BrdU+ cells, 1 = 1-49% BrdU+ cells, 2 = 50-99% BrdU+ cells, and 3 = 100% BrdU+ cells per organoid. Representative BrdU scoring system is depicted on right. **(E)** Representative immunoblot for SEMA7A and GAPDH in MCF7 cell transfected with a with scrambled control (Scr) or shSEMA7A knockdown (KD1 and KD2) constructs. Normalized quantifications are shown below. **(F)**. Confluence of Scr, KD1, or KD2 MCF7 cells at 24, 48, and 72 hours post seeding (n = 3). **(G)** Clonogenicity of Scr, KD1, or KD2 MCF7 cells. KD1 and KD2 values are normalized to Scr controls (n = 3). **(H)** BrdU incorporation was assessed in Scr, KD1, or KD2 MCF7 cells embedded in Matrigel plus 20% collagen after 10 days in culture. Scoring system as described in panel D. *p < 0.05, **p<0.01, ***p < 0.005, ****p < 0.001 by unpaired two-tailed t-test (B-D) or ANOVA with Tukey's multiple comparison test (F-H)

Kaplan Meier analysis of patients treated with tamoxifen revealed high expression of *SEMA7A* correlated with decreased relapse free survival (Figure 4A). To determine if tamoxifen was ineffective for SEMA7A expressing cells, we cultured MCF7 SEMA7A OE cells in the presence of 4-hydroxytamoxifen. We sought to determine an effective (IC50) dose of 4-hydroxytamoxifenin both EV and OE cells, and we identified a dose, 5μM, that decreased EV cell viability in full serum and in estrogen depleted conditions (SFigure 3A-B). We observed that SEMA7A OE cells grew significantly better than EV controls with 4-hydroxytamoxifen treatment (Figure 4B; SFigure 3C). We also performed a drug titration for fulvestrant and identified 7.5nM as sufficient to decrease MCF7 EV growth (SFigure 3D). We then applied this dose to SEMA7A OE cells. These fulvestrant-treated SEMA7A OE cells grew as well as vehicle-treated EV controls over time and in clonogenic assays (Figure 4C-D; SFigure 4A-B). Additionally, exogenous SEMA7A increased clonogenic outgrowth of both MCF7 and T47D

366 cells, despite the presence of fulvestrant (Figure 4E; SFigure 4C). We further observed that
367 MCF7 SEMA7A OE cells can grow *in vitro* in estrogen depleted conditions (SFigure 4D-E). We
368 next tested how SEMA7A OE tumors grow *in vivo* with endocrine therapy treatments. We
369 chose fulvestrant as we were able to achieve an IC50 dose in the presence of estrogen
370 (SFigure 3D). We implanted MCF7 EV and SEMA7A OE, cells, allowed tumors to establish,
371 then began administering fulvestrant when the tumors reached 200mm^3. Fulvestrant slowed
372 the growth of control tumors, while the SEMA7A OE tumors continued to grow at the same rate
373 (Figure 4F; SFigure 4F). At study completion, we verified SEMA7A overexpression by
374 immunohistochemistry (IHC; SFigure 5A). Consistent with a drug resistant phenotype,
375 SEMA7A OE tumors exhibited increased proliferation as measured by Ki67 staining at study
376 completion (Figure 4G; SFigure 5B) and were overall less necrotic (Figure 4H; SFigure 5C).
377 Interestingly, ER+ tumor metastases frequently lose expression of ER under conditions of
378 long-term estrogen deprivation (28), and our SEMA7A OE tumors exhibited decreased ER
379 staining intensity by semi-quantitative IHC (Figure 4I-J), which could be a sign of ER
380 independence and explain the lack of response to fulvestrant. Furthermore, *ESR1* and *PGR*—
381 a known ER target gene—downregulation were confirmed in our MCF7 SEMA7A OE cells
382 (SFigure 5D). These results suggest that SEMA7A expression in ER+BC cells renders them
383 less reliant on ER signaling for growth, which also renders them resistant to endocrine therapy
384 and able to disseminate and seed metastases in the presence of tamoxifen, AIs, or fulvestrant.
385 Consistent with this, we observe increased lung metastasis in the SEMA7A OE group (Figure
386 K-L).

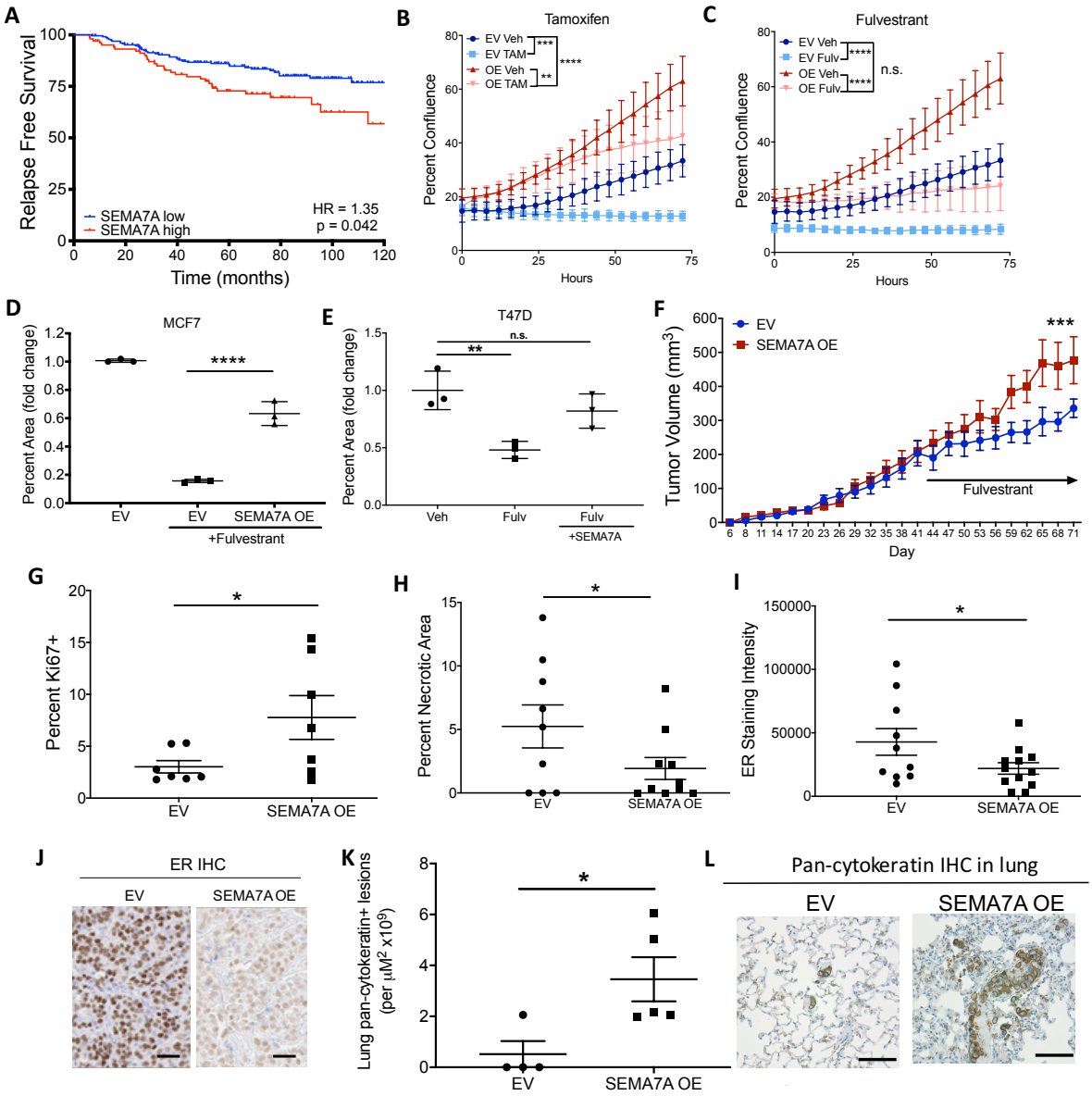

Figure 4: SEMA7A promotes endocrine resistance *in vitro* and *in vivo*. (A) Relapse free survival curves for patients with ER+ disease treated with tamoxifen are stratified by high *SEMA7A* (red) and low *SEMA7A* (blue) using KMplotter mRNA gene chip data (n = 335). **(B)** Confluence of MCF7 EV or SEMA7A OE cells treated with 5μM 4-hydroxytamoxifen (n = 3) or **(C)** 7.5nM fulvestrant (n = 3). **(D)** Clonogenic growth of EV or SEMA7A OE MCF7 cells treated with 7.5nM fulvestrant or vehicle. Fulvestrant-treated values are normalized to EV vehicle controls (n = 3). **(E)** Clonogenic growth of T47D cells treated with 7.5nM fulvestrant and 5μg/mL exogenous SEMA7A. Fulvestrant-treated values are normalized to vehicle controls (n = 3). **(F)** Tumor volumes for EV or SEMA7A OE MCF7 tumors in hosts treated with fulvestrant when tumors reached an average of 200mm^3 (n = 8-10/group). **(G)** Quantification of Ki67, **(H)** necrotic area, and **(I)** ER staining in EV or SEMA7A OE MCF7 tumors in hosts treated with fulvestrant. **(J)** Representative images of ER staining in EV or SEMA7A OE MCF7 tumors. Scale bars 25 μm. **(K)** Quantification and **(L)** representative IHC for pan-cytokeratin in lungs from mice with MCF7 EV or SEMA7A OE tumors (n = 4-6 per group). Scale bars 50 μm. *p < 0.05, **p<0.01, ***p < 0.005, ****p < 0.001 by unpaired t-test (D-I, K) or repeated measures one-way ANOVA with Tukey's multiple comparison test (B-C)

SEMA7A induces pro-metastatic phenotypes in ER+ breast cancer cells

Our previous results in ER-BC cells show that SEMA7A induces mesenchymal phenotypes (15), and SEMA7A OE in ER+ MCF7 cells resulted in cells adapting a more mesenchymal

391 morphology (SFigure 5E). We also observed increased invasion of SEMA7A OE MCF7 cells in
392 a transwell filter assay (Figure 5A). We next utilized the 3D model described above where we
393 previously demonstrated that SEMA7A promotes invasion of ER- tumor cells (9,19). Consistent
394 with our hypothesis, SEMA7A OE cells exhibited evidence of invasion as early as 5 days post
395 seeding, when most organoids in the control group remained in rounded, non-invasive
396 spheroid structures (Figure 5B). Conversely, evidence of organoids with invasive protrusions
397 appeared after 10 days in the control cells and were significantly less abundant in SEMA7A
398 knockdowns (Figure 5C).

399 After local invasion and intravasation, metastatic tumor cells exit the primary site and survive in
400 non-adherent conditions, which would induce death of normal epithelial cells via a process
401 termed “anoikis” (29). Thus, we utilized forced suspension cultures to determine whether
402 SEMA7A is upregulated in non-adherent conditions. We observed highest SEMA7A
403 expression after 72 hours in suspension, suggesting that SEMA7A may be required for anoikis
404 resistance (Figure 5D). To determine if SEMA7A expression promotes cell survival in forced
405 suspension conditions, we measured cell death via cleaved caspase 7 to reveal decreased cell
406 death in SEMA7A OE cells (Figure 5E). In contrast, KD cells showed a ~2-fold increase in cell
407 death in both attached and forced suspension conditions (Figure 5F), suggesting that
408 SEMA7A may mediate protection from cell death both at the primary site and in circulation
409 during metastasis. Collectively, these data suggest that SEMA7A expression promotes local
410 invasion and cell survival in circulation. This may be one mechanism by which SEMA7A
411 promotes relapse in patients.

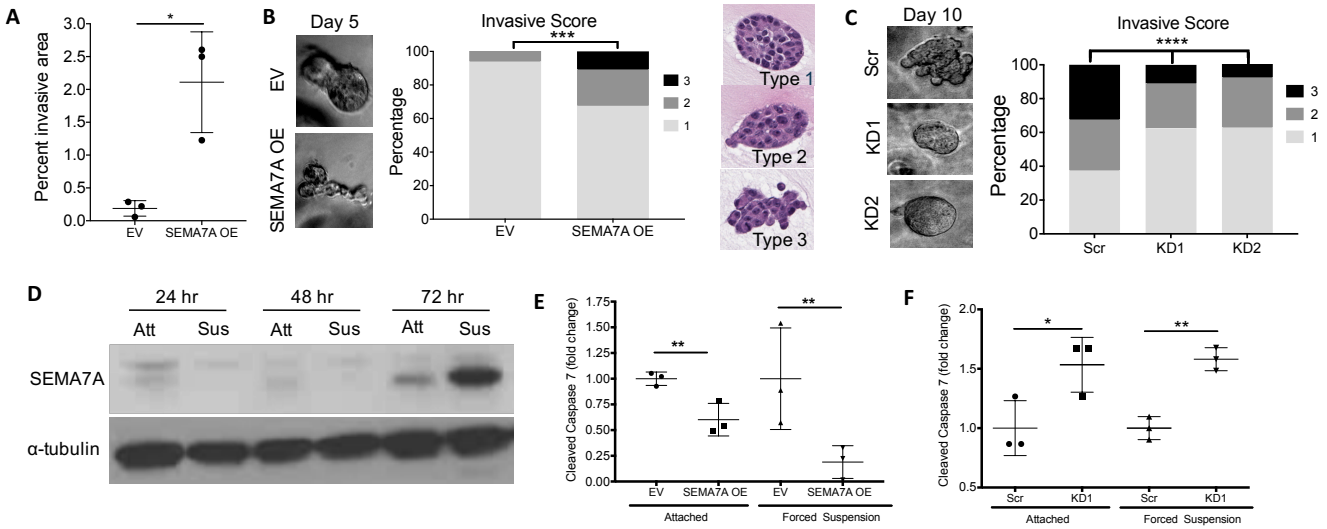

Figure 5: SEMA7A promotes metastatic phenotypes. (A))Percent invasive area is reported from MCF7 EV and SEMA7A OE cells seeded in a transwell invasion assay (n = 3). **(B)** MCF7 EV and SEMA7A OE cells embedded in Matrigel plus 20% collagen scored for invasive phenotypes after 5 days in 3D culture. Type 1 represents non-invasive organoids, type 2 represents moderately invasive organoids, and type 3 represents highly invasive organoids. Representative live images (left), quantification (middle), and H&Es of typing system right) are shown. **(C)** MCF7 Scr, KD1, or KD2 cells embedded in Matrigel plus 20% collagen scored for invasive phenotypes after 10 days in 3D culture. Representative live images (left) and quantification (right) are shown. **(D)** Immunoblot for SEMA7A in wildtype MCF7 cells cultured in normal attached (Att) or forced suspension (Sus) conditions over a timecourse (n = 3). **(E)** Cleaved caspase 7 activity in MCF7 EV and SEMA7A OE (n = 3) or **(F)** Scr and KD1 cells grown in attached or forced suspension cultures for 48 hours (n = 3). Data normalized to EV or Scr controls in attached conditions. *p < 0.05, **p<0.01, ***p < 0.005, ****p < 0.001 by unpaired two-sided t-test (A-B) or one-way ANOVA with Tukey's multiple comparison test (C, E-F)

Therapeutic vulnerability of SEMA7A-expressing ER+ tumor cells

Based on our observation that SEMA7A drives growth and metastasis of ER+ tumors and are resistant to endocrine therapy, we postulated that CDK 4/6 inhibitors, which have recently been approved and proven effective for patients with metastatic ER+BC, could inhibit growth of SEMA7A expressing cells. As expected, when treated with 2.5μM of the CDK 4/6 inhibitor palbociclib, MCF7 EV control cells exhibited a significant reduction of growth and clonogenicity *in vitro* compared to vehicle treatment; however, SEMA7A OE cells grew significantly better with palbociclib treatment (Figure 6A-B; SFigure 6A). We therefore sought to identify therapies that may have efficacy for treating patients with SEMA7A-expressing tumors. Using an Oncomine query to identify potential compounds and targetable pathways, we identified 6 compounds predicted to elicit sensitivity of SEMA7A+ tumors, all of which target proteins in either the MAPK or PI3K/AKT signaling pathways (STable 4). Notably, published studies describe these pathways as downstream signaling mediators of SEMA7A activity (2,5,8). Thus, we tested whether growth of SEMA7A OE cells is inhibited by commercially available small molecule inhibitors that target Src and Akt, SU6656 and LY294002, respectively. We observed significantly decreased growth of SEMA7A OE cells with both inhibitors (SFigure 6B-C).

429 However, as these compounds are not clinically available, we sought to identify a compound
430 that would inhibit the downstream pro-survival function induced by these pathways. Venetoclax
431 is an orally available inhibitor of the anti-apoptotic BCL2 protein that has recently demonstrated
432 synergy in combination therapy approaches in patients with ER+BC (30). We first identified
433 that our cells expressed BCL2 and observed increased expression in SEMA7A OE cells
434 (Figure 6C). Then, we tested the sensitivity of SEMA7A OE cells to venetoclax at a clinically
435 relevant dose. Proliferation of SEMA7A OE cells was decreased with venetoclax treatment as
436 compared to vehicle treatment and to EV control cells treated with venetoclax, while
437 clonogenic outgrowth was decreased in both EV and SEMA7A OE cells (Figure 6D-E and
438 SFigure 6D). To test whether fulvestrant resistant SEMA7A OE tumors respond to venetoclax
439 treatment *in* vivo, we implanted MCF7 EV control or SEMA7A OE cells into NCG mice. Tumors
440 were allowed to grow to an average of 200mm^3, when we then initiated fulvestrant treatment.
441 As expected, the SEMA7A OE tumors continued to grow, while tumor growth plateaued in the
442 control group. After separation of the curves was observed, we administered vehicle or
443 venetoclax treatment in combination with fulvestrant. We observed a dramatic decrease in
444 tumor growth, tumor growth rate, final tumor volume, and decreased Ki67+ tumor cells in the
445 SEMA7A OE, which was surprisingly not observed in the EV control group (Figure 6F-H and
446 SFigure 6E&F). Next, we sought to examine whether BCL2 expression was affected by the
447 fulvestrant treatment, as BCL2 is an ER target gene. To this end, we harvested cells from
448 fulvestrant treated tumors and cultured them *ex vivo* in the presence of fulvestrant (SFigure
449 7A-B). Immunoblot analysis of these cells revealed that the fulvestrant resistant EV (FR-EV)
450 cells lost expression of BCL2, while the fulvestrant resistant SEMA7A OE (FR-OE) cells
451 maintained expression (Figure 6I). Additionally, the FR-OE cells were enriched for
452 CD44+CD24- cell populations (Figure 6J; SFigure 8A-C), which exhibit increased capacity for
453 self-renewal, generation of heterogenous progeny, enhanced invasive phenotypes and drug
454 resistance (31,32); these results suggest that SEMA7A OE may result in enrichment for drug
455 resistant stem cells in response to endocrine therapy, which may also promote metastasis. To
456 determine whether there is potential for venetoclax to prevent metastasis of SEMA7A+ER+
457 tumors, we measured lung metastasis in our co-treated animals and found a significant
458 decrease with the addition of venetoclax to fulvestrant treatment (Figure 6K). Thus, our results
459 suggest that venetoclax may be an viable treatment option for inhibiting growth, recurrence,

and metastasis of SEMA7A-expressing ER+BCs, which are likely to be resistant to endocrine therapies.

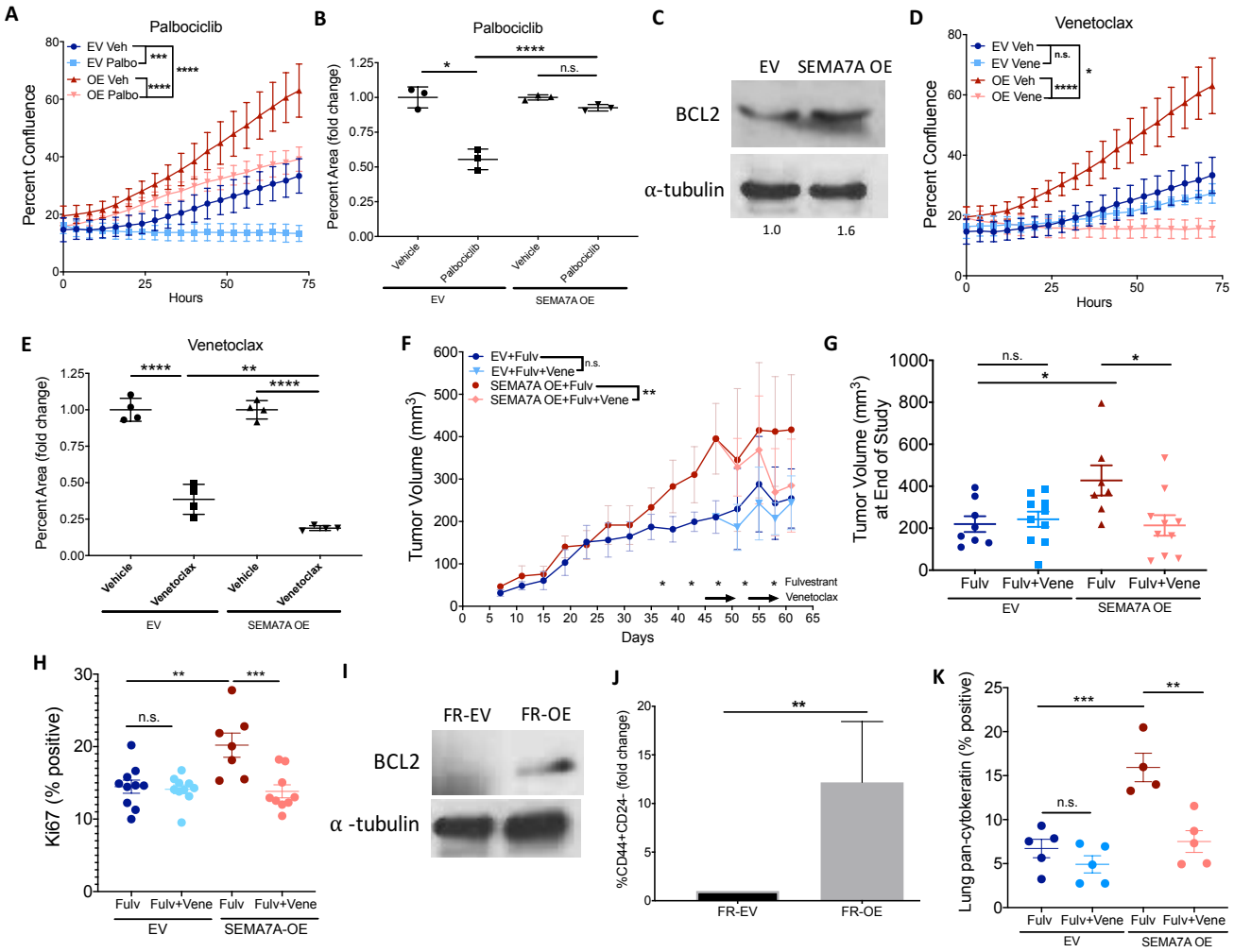

Figure 6: Therapeutic vulnerability of SEMA7A-expressing tumors. (A) Confluence and **(B)** clonogenic growth of MCF7 EV or SEMA7A OE cells treated with 2.5μM palbociclib. Clonogenic data are normalized to vehicle controls (n = 3). **(C)** Representative immunoblot of BCL2 and α-tubulin are shown for MCF7 EV and SEMA7A OE cells (n = 3). Normalized quantification is below. **(D)** Confluence and **(E)** clonogenic growth of MCF7 EV or SEMA7A OE cells treated with 300nM venetoclax. Clonogenic data are normalized to vehicle controls (n = 3). **(F)** Tumor volumes of MCF7 EV and SEMA7A OE tumors in hosts treated with fulvestrant +/- venetoclax (n = 4/group). **(G)** Individual tumor volumes of MCF7 EV and SEMA7A OE tumors at end of study after fulvestrant +/- venetoclax treatment. Data are pooled from 2 independent studies. **(H)** Ki67 analysis of MCF7 EV and SEMA7A OE tumors treated with fulvestrant +/- venetoclax. Data are pooled from 2 independent studies. **(I)** Representative immunoblot of BCL2 and α-tubulin are shown for MCF7 fulvestrant resistant (FR) EV and SEMA7A OE cells (n = 3). **(J)** Flow cytometry analysis of MCF7 FR-EV and FR-OE cells. Data are normalized to FR-EV condition. **(K)** Quantification of pan-cytokeratin in lungs from mice with MCF7 EV or SEMA7A OE tumors that were treated with fulvestrant +/- venetoclax. Data pooled from 2 independent studies. *p < 0.05, **p<0.01, ***p < 0.005, ****p < 0.001 by one-way ANOVA with Tukey's multiple comparison test (B,E-H,K) or repeated measures one-way ANOVA with Tukey's multiple comparison test (A,D)

DISCUSSION

Determining whether patients with ER+BC will or will not respond to endocrine therapy and identifying novel treatment options for patients with endocrine resistant ER+BC is of the utmost importance, as patients with ER+ disease comprise the largest percentage of BC patients and

468 the largest number of BC-related deaths. The semaphorin family of proteins have multiple, and
469 variable, described roles in cancer, with some demonstrating tumor-suppressive functions and
470 others demonstrating tumor-promotional roles (33). The data presented in this study contribute
471 to an emerging body of evidence describing a role for SEMA7A in tumor progression. Our lab
472 and others have recently begun to characterize SEMA7A as a mediator of breast/mammary,
473 melanoma, and lung cancer (9-14). In this report, we describe a novel role for SEMA7A in
474 ER+BC recurrence and metastasis, where SEMA7A expression confers resistance to anti-
475 endocrine therapy and predicts for poor response in patients with ER+ disease. In previously
476 published data, we showed that SEMA7A promotes numerous tumor-promotional phenotypes
477 in ER- preclinical models, including tumor cell growth, motility, invasion, and cell survival
478 (9,15). We also reported that SEMA7A induces macrophage-mediated remodeling of lymphatic
479 vasculature, as well as tumor cell dissemination via the lymphatics, and others have
480 demonstrated SEMA7A-dependent angiogenesis in ER-BC models (10,11).
481
482 Motility and invasion are known hallmarks of metastatic cells (29). However, as cells venture
483 through the metastatic cascade, they must also adapt to many different microenvironments
484 such as certain hostile conditions, including anchorage independent conditions during travel
485 through the vasculature or lymphatics. We now show that SEMA7A expression promotes
486 anoikis resistance and consequent anchorage-independent survival and we extend our
487 observations to show that SEMA7A overexpression can promote spontaneous and
488 experimental lung metastasis. Additionally, we suggest that the pleiotropic effects promoted by
489 SEMA7A may give SEMA7A-expressing tumors a selective advantage under the stress of
490 endocrine therapies, which results in long-term hormonal depravation intended to halt tumor
491 cell growth and induce cell death. Our results support that SEMA7A expression allows tumor
492 cells to bypass reliance on ER, rendering them reliant instead upon SEMA7A mediated cell
493 survival. This is further evidenced by our observations that SEMA7A-expressing tumors
494 downregulate expression of ER—a mechanism that warrants further investigation.
495 Furthermore, published studies report that SEMA4C promotes MCF7 tumor growth, viability,
496 metastasis, and renders ER+ cells non-responsive to tamoxifen via downregulation of ER (34),
497 suggesting that this mechanism may extend to other multiple semaphorin family members.
498

499 Metastatic disease in patients with ER+BC frequently exhibits endocrine resistance, and many
500 metastases downregulate ER or express mutant forms of the *ESR1* gene. Although the
501 prevalence of ER loss has been debated, a recent meta-analysis reveals approximately 23%
502 of ER+ tumors have corresponding ER- metastases (28). Further, tumors with low expression
503 of ER (1-10% positive) are reported to behave more like ER- tumors, and patients with ER low
504 tumors have significantly lower disease free survival rates compared to patients with ER high
505 (11-100% positive) tumors (35). These results are consistent with our observations that
506 SEMA7A expressing cells exhibit pro-metastatic phenotypes and are also resistance to
507 therapy and downregulate ER. We suggest that initial expression of SEMA7A in hormone
508 receptor positive disease is promoted cooperation between ER and SP1 at the SEMA7A
509 promoter, as we demonstrate that SEMA7A expression can be promoted by estrogen
510 treatment in a dose-dependent manner and that both the ERE half sites and SP1 sites are
511 required for induction of promoter activity by estrogen. However, SEMA7A expression is not
512 completely inhibited with ER degradation in ER+BC cells, suggesting additional mechanisms
513 are at play to regulate SEMA7A expression. Studies of other semaphorins have described
514 hormone receptor regulation. In ovarian cancer, pro-proliferative *SEMA4D* is positively
515 regulated by ER (36). Conversely, expression of *SEMA3B* and *SEMA3F*, which are both
516 growth-suppressive, in ovarian cancer is positively regulated by E2 and progesterone (37).
517 Finally, *SEMA3C* is transcriptionally regulated by the androgen receptor (AR) in prostate
518 cancer cells (38) and promotes growth, migration, and invasion in BC (39), is detectable in
519 metastatic lung cancer cells (40), and promotes survival of gastric cancer and glioma stem
520 cells (41,42). SEMA3C also has a described role in promoting drug resistance in ovarian
521 cancer (43). Consistent with a mechanism for SEMA7A in drug resistance, our observation that
522 ER levels in SEMA7A OE tumors are decreased after fulvestrant treatment suggests that
523 fulvestrant had the intended effect, but that fulvestrant alone was not sufficient to control
524 growth in SEMA7A expressing tumors, suggesting a bypass mechanism. Taken together,
525 these studies support that future investigations, utilizing chromatin immunoprecipitation, will be
526 necessary to show direct promoter binding of SEMA7A by multiple nuclear hormone receptors,
527 including ER, PR and AR.
528

529 In addition to endocrine therapy resistance, we demonstrate that SEMA7A expression confers
530 resistance to the CDK 4/6 inhibitor palbociclib, which is used in combination with endocrine
531 therapy for first line treatment of metastatic disease or in subsequent lines following disease
532 progression (44). Our data suggest that patients with SEMA7A+ tumors may be at high risk for
533 relapse and poor response to current standard-of-care therapies, and that novel therapeutic
534 strategies could be applied for patients pre-selected by SEMA7A status. Interestingly,
535 Kinehara et al. recently described that SEMA7A promotes resistance to standard-of-care
536 EGFR tyrosine kinase inhibitors in lung cancer through anti-apoptotic β1-integrin-mediated
537 ERK signaling; SEMA7A was thus proposed as a predictive marker for response to TKI
538 therapy and potential therapeutic target for resistant tumors (14). This report, along with our
539 findings, suggests that SEMA7A may confer resistance to multiple targeted therapies in
540 numerous tumor types; therefore, direct targeting and therapeutic vulnerabilities of SEMA7A+
541 tumors warrant additional investigation in a clinical setting. Moving toward this goal, results
542 presented herein suggest that SEMA7A+ tumors may be targetable via other mechanisms.
543 Specifically, SEMA7A has demonstrated the ability to activate PI3K/AKT and MAPK/ERK
544 signaling (2,5,8). We now report that SEMA7A OE cells have increased expression of the anti-
545 apoptotic protein BCL2. We therefore tested if SEMA7A+ tumor cells exhibit sensitivity to
546 selective inhibitors of these pathways, including the BCL2 inhibitor venetoclax. Our results
547 showing that SEMA7A+ tumors cells exhibit reduced growth and viability after exposure to
548 these therapeutics support that targeting downstream effectors of SEMA7A may prove an
549 effective strategy for recurrent SEMA7A+ tumors, which are resistant to currently available
550 therapeutic regimes. We also show, for the first time, that when treated with fulvestrant,
551 SEMA7A expressing tumors maintain expression of BCL2 while controls lose BCL2
552 expression. Previous reports have described increased BCL2 expression in fulvestrant-
553 resistant MCF7 cells, and fulvestrant sensitivity can be restored with a BCL2 inhibitor or BCL2
554 knockdown (45). Additionally, the first clinical study of the BCL2 inhibitor venetoclax in solid
555 tumors revealed that patients with metastatic ER+BC received great benefit from this drug in
556 combination with tamoxifen, and a recent report describes a benefit of adding venetoclax to
557 fulvestrant/palbociclib in preclinical ER+ models (46). While we have not explored this triple
558 combination in our current studies, future studies will explore whether venetoclax can reverse
559 the resistance to palbociclib that we observe in our SEMA7A OE cells. Since venetoclax is

clinically available, administered orally, and well-tolerated, we propose that novel clinical trials could test whether patients with ER+SEMA7A+ cancer would benefit from combination treatment in both the adjuvant and metastatic setting. Finally, clinical trials assessing SEMA4C as a biomarker for BC diagnosis and relapse are already underway (ClinicalTrials.gov identifiers: NCT03663153 and NCT03662633). Since similar phenotypes are observed in pre-clinical models with SEMA4C and SEMA7A, we propose that SEMA7A may also warrant investigation in the clinic as a predictive marker of ER+BC recurrence.

ACKNOWLEDGEMENTS

The authors acknowledge the CU Anschutz Cancer Center Protein Production/MoAB/Tissue Culture Shared Resource, the Biorepository Core Facility, and the University of Colorado Cancer Center Support Grant (P30CA046934) for SEMA7A protein production, Incucyte use, and Aperio Software use. Contents are the authors' sole responsibility and do not necessarily represent official NIH views. The authors also thank the following persons for technical support and feedback in the production of this manuscript: Alan Elder, Alexander Stoller, Veronica Wessells, Michelle Borakove, Virginia Borges, Chloe Young, Sarah Tarullo, Annie Pham, Paris Franz, Craig Jordan, and Brett Stevens.

Author Contributions:

LSC and TRL conceived and designed the study. LSC performed all *in vivo* studies. LSC, GLW, and TRR performed all *in vitro* studies. JKR and WWP assisted with methodology development and data interpretation. GLW, WWP, and JKR provided critical reagents. LSC and TRL were responsible for hypothesis development, conceptual design, and data analysis. LSC and TRL wrote the manuscript, and all authors provided critical evaluation, editing, and review of the manuscript.

REFERENCES

1. Pan H, Gray R, Braybrooke J, Davies C, Taylor C, McGale P*, et al.* 20-Year Risks of Breast-Cancer Recurrence after Stopping Endocrine Therapy at 5 Years. N Engl J Med **2017**;377:1836-46

591 2. Pasterkamp RJ, Peschon JJ, Spriggs MK, Kolodkin AL. Semaphorin 7A promotes axon
592 outgrowth through integrins and MAPKs. Nature **2003**;424:398-405
593 3. Mine T, Harada K, Matsumoto T, Yamana H, Shirouzu K, Itoh K*, et al.* CDw108 expression
594 during T-cell development. Tissue Antigens **2000**;55:429-36
595 4. Zhang M, Wang L, Dong M, Li Z, Jin F. Endothelial Semaphorin 7A promotes inflammation in
596 seawater aspiration-induced acute lung injury. Int J Mol Sci **2014**;15:19650-61
597 5. Suzuki K, Okuno T, Yamamoto M, Pasterkamp RJ, Takegahara N, Takamatsu H*, et al.*
598 Semaphorin 7A initiates T-cell-mediated inflammatory responses through alpha1beta1 integrin.
599 Nature **2007**;446:680-4
600 6. Morote-Garcia JC, Napiwotzky D, Kohler D, Rosenberger P. Endothelial Semaphorin 7A
601 promotes neutrophil migration during hypoxia. Proc Natl Acad Sci U S A **2012**;109:14146-51
602 7. Parkash J, Messina A, Langlet F, Cimino I, Loyens A, Mazur D*, et al.* Semaphorin7A regulates
603 neuroglial plasticity in the adult hypothalamic median eminence. Nat Commun **2015**;6:6385
604 8. Kang H-R, Lee CG, Homer RJ, Elias Ja. Semaphorin 7A plays a critical role in TGF-beta1-
605 induced pulmonary fibrosis. The Journal of experimental medicine **2007**;204:1083-93
606 9. Black SA, Nelson AC, Gurule NJ, Futscher BW, Lyons TR. Semaphorin 7a exerts pleiotropic
607 effects to promote breast tumor progression. Oncogene **2016**;35:5170-8
608 10. Elder AM, Tamburini BAJ, Crump LS, Black SA, Wessells VM, Schedin PJ*, et al.* Semaphorin
609 7A Promotes Macrophage-Mediated Lymphatic Remodeling during Postpartum Mammary
610 Gland Involution and in Breast Cancer. Cancer Res **2018**;78:6473-85
611 11. Garcia-Areas R, Libreros S, Amat S, Keating P, Carrio R, Robinson P*, et al.* Semaphorin7A
612 promotes tumor growth and exerts a pro-angiogenic effect in macrophages of mammary tumor-
613 bearing mice. Frontiers in physiology **2014**;5:17
614 12. Ma B, Herzog EL, Lee CG, Peng X, Lee CM, Chen X*, et al.* Role of chitinase 3-like-1 and
615 semaphorin 7a in pulmonary melanoma metastasis. Cancer Res **2015**;75:487-96
616 13. Garcia-Areas R, Libreros S, Simoes M, Castro-Silva C, Gazaniga N, Amat S*, et al.* Suppression
617 of tumor-derived Semaphorin 7A and genetic ablation of host-derived Semaphorin 7A impairs
618 tumor progression in a murine model of advanced breast carcinoma. Int J Oncol **2017**;51:1395-
619 404
620 14. Kinehara Y, Nagatomo I, Koyama S, Ito D, Nojima S, Kurebayashi R*, et al.* Semaphorin 7A
621 promotes EGFR-TKI resistance in EGFR mutant lung adenocarcinoma cells. JCI Insight **2018**;3
622 15. Tarullo SE, Hill RC, Hansen KC, Behbod F, Borges VF, Nelson AC*, et al.* Postpartum breast
623 cancer progression is driven by semaphorin 7a-mediated invasion and survival. Oncogene **2020**
624 16. Seth P, Krop I, Porter D, Polyak K. Novel estrogen and tamoxifen induced genes identified by
625 SAGE (Serial Analysis of Gene Expression). Oncogene **2002**;21:836-43
626 17. Xiao T, Li W, Wang X, Xu H, Yang J, Wu Q*, et al.* Estrogen-regulated feedback loop limits the
627 efficacy of estrogen receptor-targeted breast cancer therapy. Proceedings of the National
628 Academy of Sciences of the United States of America **2018**;115:7869-78
629 18. Seth P, Porter D, Lahti-Domenici J, Geng Y, Richardson A, Polyak K. Cellular and Molecular
630 Targets of Estrogen in Normal Human Breast Tissue. Cancer research **2002**;62:4540-4
631 19. Lyons TR, O'Brien J, Borges VF, Conklin MW, Keely PJ, Eliceiri KW*, et al.* Postpartum
632 mammary gland involution drives progression of ductal carcinoma in situ through collagen and
633 COX-2. Nat Med **2011**;17:1109-15
634 20. DeRose YS, Gligorich KM, Wang G, Georgelas A, Bowman P, Courdy SJ*, et al.* Patient-derived
635 models of human breast cancer: protocols for in vitro and in vivo applications in tumor biology
636 and translational medicine. Curr Protoc Pharmacol **2013**;Chapter 14:Unit14 23
637 21. O'Brien J, Lyons T, Monks J, Lucia MS, Wilson RS, Hines L*, et al.* Alternatively activated
638 macrophages and collagen remodeling characterize the postpartum involuting mammary gland
639 across species. Am J Pathol **2010**;176:1241-55
640 22. Nagy A, Lanczky A, Menyhart O, Gyorffy B. Validation of miRNA prognostic power in
641 hepatocellular carcinoma using expression data of independent datasets. Sci Rep **2018**;8:9227

642 23. Soule HD, Maloney TM, Wolman SR, Peterson WD, Jr., Brenz R, McGrath CM*, et al.* Isolation
643 and characterization of a spontaneously immortalized human breast epithelial cell line, MCF-10.
644 Cancer research **1990**;50:6075-86
645 24. Stanczyk FZ, Clarke NJ. Measurement of estradiol--challenges ahead. J Clin Endocrinol Metab
646 **2014**;99:56-8
647 25. Kreft L, Soete A, Hulpiau P, Botzki A, Saeys Y, De Bleser P. ConTra v3: a tool to identify
648 transcription factor binding sites across species, update 2017. Nucleic Acids Res
649 **2017**;45:W490-W4
650 26. Porter W, Saville B, Hoivik D, Safe S. Functional synergy between the transcription factor Sp1
651 and the estrogen receptor. Mol Endocrinol **1997**;11:1569-80
652 27. Lyons TR, O'Brien J, Borges VF, Conklin MW, Keely PJ, Eliceiri KW*, et al.* Postpartum
653 mammary gland involution drives progression of ductal carcinoma in situ through collagen and
654 COX-2. Nature medicine **2011**;17:1109-15
655 28. Schrijver W, Suijkerbuijk KPM, van Gils CH, van der Wall E, Moelans CB, van Diest PJ.
656 Receptor Conversion in Distant Breast Cancer Metastases: A Systematic Review and Meta-
657 analysis. Journal of the National Cancer Institute **2018**;110:568-80
658 29. Welch DR, Hurst DR. Defining the Hallmarks of Metastasis. Cancer Res **2019**;79:3011-27
659 30. Lok SW, Whittle JR, Vaillant F, Teh CE, Lo LL, Policheni AN*, et al.* A Phase Ib Dose-Escalation
660 and Expansion Study of the BCL2 Inhibitor Venetoclax Combined with Tamoxifen in ER and
661 BCL2-Positive Metastatic Breast Cancer. Cancer Discov **2019**;9:354-69
662 31. Sheridan C, Kishimoto H, Fuchs RK, Mehrotra S, Bhat-Nakshatri P, Turner CH*, et al.*
663 CD44+/CD24-breast cancer cells exhibit enhanced invasive properties: an early step necessary
664 for metastasis. Breast Cancer Research **2006**;8:R59
665 32. Dean M, Fojo T, Bates S. Tumour stem cells and drug resistance. Nature Reviews Cancer
666 **2005**;5:275-84
667 33. Neufeld G, Mumblat Y, Smolkin T, Toledano S, Nir-Zvi I, Ziv K*, et al.* The role of the
668 semaphorins in cancer. Cell Adh Migr **2016**;10:652-74
669 34. Gurrapu S, Pupo E, Franzolin G, Lanzetti L, Tamagnone L. Sema4C/PlexinB2 signaling controls
670 breast cancer cell growth, hormonal dependence and tumorigenic potential. Cell Death Differ
671 **2018**;25:1259-75
672 35. Prabhu JS, Korlimarla A, Desai K, Alexander A, Raghavan R, Anupama C*, et al.* A Majority of
673 Low (1-10%) ER Positive Breast Cancers Behave Like Hormone Receptor Negative Tumors. J
674 Cancer **2014**;5:156-65
675 36. Liu Y, Hou Y, Ma L, Sun C, Pan J, Yang Y*, et al.* Regulation of semaphorin 4D expression and
676 cell proliferation of ovarian cancer by ERalpha and ERbeta. Braz J Med Biol Res **2017**;50:e6057
677 37. Joseph D, Ho SM, Syed V. Hormonal regulation and distinct functions of semaphorin-3B and
678 semaphorin-3F in ovarian cancer. Mol Cancer Ther **2010**;9:499-509
679 38. Tam KJ, Dalal K, Hsing M, Cheng CW, Khosravi S, Yenki P*, et al.* Androgen receptor
680 transcriptionally regulates semaphorin 3C in a GATA2-dependent manner. Oncotarget
681 **2017**;8:9617-33
682 39. Esselens C, Malapeira J, Colome N, Casal C, Rodriguez-Manzaneque JC, Canals F*, et al.* The
683 cleavage of semaphorin 3C induced by ADAMTS1 promotes cell migration. J Biol Chem
684 **2010**;285:2463-73
685 40. Martin-Satue M, Blanco J. Identification of semaphorin E gene expression in metastatic human
686 lung adenocarcinoma cells by mRNA differential display. J Surg Oncol **1999**;72:18-23
687 41. Miyato H, Tsuno NH, Kitayama J. Semaphorin 3C is involved in the progression of gastric
688 cancer. Cancer Sci **2012**;103:1961-6
689 42. Man J, Shoemake J, Zhou W, Fang X, Wu Q, Rizzo A*, et al.* Sema3C promotes the survival and
690 tumorigenicity of glioma stem cells through Rac1 activation. Cell Rep **2014**;9:1812-26
691 43. Yamada T, Endo R, Gotoh M, Hirohashi S. Identification of semaphorin E as a non-MDR drug
692 resistance gene of human cancers. Proc Natl Acad Sci U S A **1997**;94:14713-8

693 44. Beaver JA, Amiri-Kordestani L, Charlab R, Chen W, Palmby T, Tilley A*, et al.* FDA Approval:
694 Palbociclib for the Treatment of Postmenopausal Patients with Estrogen Receptor-Positive,
695 HER2-Negative Metastatic Breast Cancer. Clin Cancer Res **2015**;21:4760-6
696 45. Crawford AC, Riggins RB, Shajahan AN, Zwart A, Clarke R. Co-inhibition of BCL-W and BCL2
697 restores antiestrogen sensitivity through BECN1 and promotes an autophagy-associated
698 necrosis. PloS one **2010**;5:e8604
699 46. Whittle JR, Vaillant F, Surgenor E, Policheni AN, Giner G, Capaldo BD*, et al.* Dual targeting of
700 CDK4/6 and BCL2 pathways augments tumor response in estrogen receptor positive breast
701 cancer. Clin Cancer Res **2020**

702